

STRUCTURAL ASPECTS OF ORGANIC SUPERCONDUCTORS

The structural properties of organic charge-transfer salts based on the electron donors tetramethyltetraselenafulvalene (TMTSF) and bis(ethylenedithiolo)tetrathiafulvalene (BEDT-TTF) and on a variety of complex inorganic anions (X) are examined systematically. For the isomorphous series of (TMTSF)₂X salts, the analysis of a variety of structural data reveals that anion size and symmetry are crucial parameters. For the structurally complex (BEDT-TTF)₂X salts, a crystallographic family tree is developed that aids in the systematization of their structural and electrical properties. A particularly illuminating aspect of the crystallographic family tree is that alternate generations are populated by salts with anions of opposite inversion symmetry. For each series of salts, structurally unique properties are identified for members that exhibit ambient-pressure superconductivity.

INTRODUCTION

In general, it is expected that the intrinsic electrical conductivity in purely organic solids will be limited (nominally to insulators) by the large covalent energy gap that stabilizes these materials. However, only a brief reflection indicates that variations in intrinsic conductivity in organic solids can be substantial and that the variations often have their antecedents in crystalline structure. For example, the allotropes (forms possessing different crystalline motifs) of carbon have dramatically different electrical behaviors. Diamond (with its cubic crystal structure) is an isotropic insulator, while graphite (with its layered hexagonal crystal structure) is an anisotropic semiconductor with an intralayer-to-interlayer conductivity ratio of about 10^3 .

About 20 years ago, researchers began to realize that, within a specific structural class of organic materials, compounds could be synthesized whose conductivities were quite substantial, even approaching those of common metals.¹ Specifically, it was demonstrated that planar molecular ions having inhomogeneous charge densities could be stacked along the direction of strong π -orbital overlaps to form an array of parallel conducting chains that were well separated from charge-balancing counterions. The anisotropic ionic gap that stabilizes these structures offers no impediment to quasi-one-dimensional band conduction along the molecular chains.

A little over a decade ago, a veritable revolution took place in the study of the electrical properties of organic solids. With the synthesis² of the charge-transfer salt of the electron donor tetrathiafulvalene (TTF) and the electron acceptor tetracyano-*p*-quinodimethane (TCNQ), the first example of a truly metallic organic solid was realized. While the solid-state physics of organic charge-transfer salts such as TTF-

TCNQ depends on a number of variables (e.g., ionization potentials of the donor, electron affinities of the acceptor, the degree of charge transferred from the donor to the acceptor, and the strength of conduction electron-phonon coupling), crystalline structure has again proven to be an essential parameter in the achievement of metallic transport. The presence of uniform segregated stacks of TTF donors and TCNQ acceptors in the crystalline structure of TTF-TCNQ³ leads to (a) highly anisotropic and weakly dispersive electronic bands formed from the frontier π -molecular orbitals of the donor and acceptor; (b) anisotropic, quasi-one-dimensional, electrical transport (often the conductivity along the columnar arrays is two to three orders of magnitude larger than in the plane normal to these arrays); and (c) an electron (spin)-phonon system that is particularly susceptible to the condensation at low temperature of charge- or spin-density waves, ultimately leading to a structural transformation and a metal-to-insulator phase transition.

This inherent instability at low temperature seemed for some time to limit the potential of low-dimensional organic charge-transfer salts to high-temperature ($T > 60$ K) metals. However, a second phase of the revolution took place about five years ago with the realization of organic superconductivity, albeit at very low temperature (about 1 K) and often requiring moderately large hydrostatic pressure (5 to 10 kilobars). Bechgaard and his colleagues⁴ prepared a series of (TMTSF)₂X salts, where TMTSF is the electron donor tetramethyltetraselenafulvalene and X is any one of a plethora of complex inorganic anions. One of the salts, (TMTSF)₂PF₆,⁵ was shown to exhibit superconductivity (at $T_c \approx 1$ K) under an applied pressure of 6 kilobars. Shortly thereafter, it was determined that a second salt, (TMTSF)₂ClO₄,⁶ became supercon-

ducting at 1.4 K, but, importantly, without the need for applied pressure. Subsequently, several other $(\text{TMTSF})_2\text{X}$ salts were added to the growing list of superconductors, but $(\text{TMTSF})_2\text{ClO}_4$ remained the lone example of an ambient-pressure superconductor.

More recently, it has been reported by several investigators⁷⁻⁹ that charge-transfer salts of the organic donor bis(ethylenedithio)tetrathiafulvalene (BEDT-TTF)¹⁰ also contain examples that display low-temperature superconductivity. Notable among these are the perrhenate salt, which requires an applied pressure of 5 kilobars,⁷ and the triiodide⁸ and dibromiodide⁹ salts, which are ambient-pressure superconductors (at $T_c \approx 1.2$ and 2.4 K, respectively). Very recently, a Japanese group¹¹ has reported that $(\text{BEDT-TTF})_2\text{I}_3$ shows a superconducting transition at 8 K at a moderate pressure of 1.3 kilobars.

The purpose of the present work is to provide an introduction to these novel superconducting organic salts, to expose some of their very interesting and systematic structural properties, and to attempt to relate their structural variability to their diverse electrical behavior. Emphasis will be focused on the role, beyond simple charge balance, of the anionic counterion X, particularly with regard to the structural and electrical consequences of variations in the size and symmetry of this counterion.

$(\text{TMTSF})_2\text{X}$ SALTS

The molecular structure of the electron donor TMTSF is presented in Fig. 1. Two features of its molecular architecture are of particular interest here. First, the four selenium atoms of the tetraselenaethylene core are instrumental in determining the inter-donor interactions in the crystal structure of the $(\text{TMTSF})_2\text{X}$ salts and the form and dimensionality of the electron bands. Second, the four terminal methyl substituents, in conjunction with the selenium atoms, comprise the structural cavity in which the anion resides.

The molecular topology of two of the anionic counterions in the $(\text{TMTSF})_2\text{X}$ salts are shown in Fig. 2. The hexafluorophosphate ion (PF_6^-) is composed of a central phosphorous ion surrounded by six fluorine ions, each ideally located at the vertex of a regular octahedron, and is characterized by the point symmetry group O_h .¹² An important symmetry element of this and other octahedral anions is their inherent centrosymmetry: any one fluorine ion can be inverted through the central phosphorus ion to yield an equivalent fluorine ion. In contrast, the perchlorate anion (ClO_4^-) is composed of a central chlorine ion surrounded by four oxygen ions, now ideally located at the vertices of a regular tetrahedron; it is characterized by the point symmetry group T_d .^{12, 13} In further contrast to the octahedral PF_6^- anion, the tetrahedral ClO_4^- anion is noncentrosymmetric. Inversion of the four terminal oxygen ions through the central chlorine ion yields four new oxygen ion positions. In total, the eight oxygen ions lie at the vertices of a regular cube. Figure 2 shows both an original (black) and an

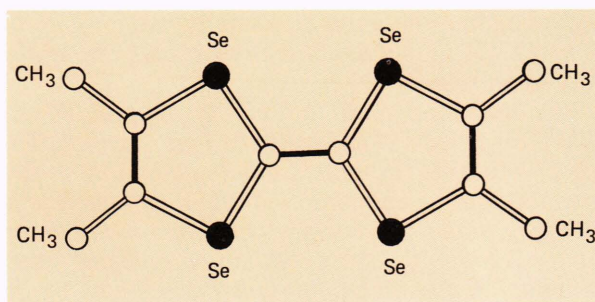


Figure 1—Molecular structure of the electron donor TMTSF. Shaded bonds indicate formal carbon-carbon double bonds.

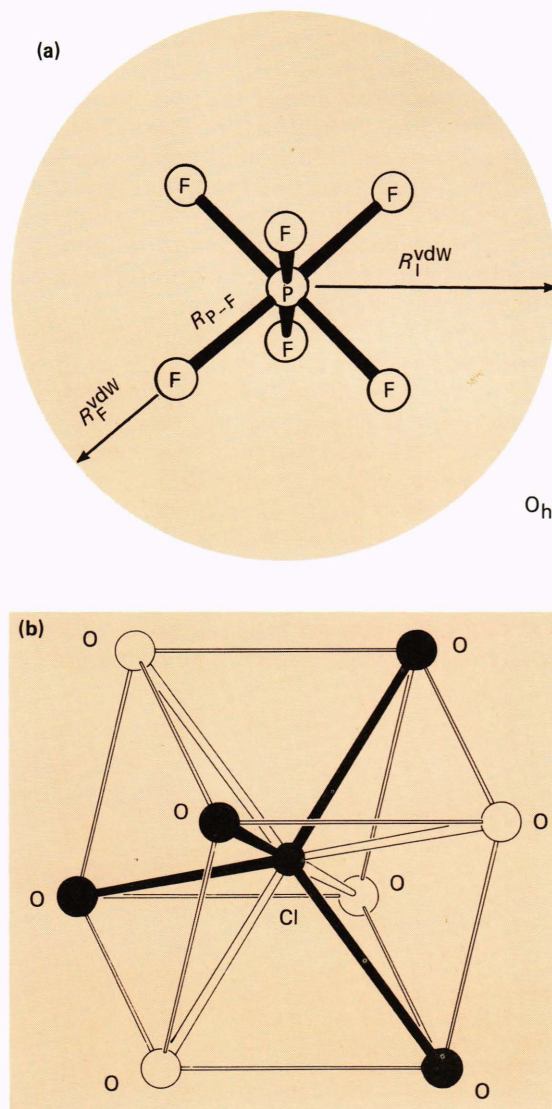


Figure 2—(a) The octahedral hexafluorophosphate (PF_6^-) anion and the trace of its van der Waals sphere of radius R_1^{vdw} . (b) Two orientations of the tetrahedral perchlorate (ClO_4^-) anion within the cube defined by its statistically disordered terminal oxygen ions.

inverted (white) perchlorate anion within a regular cube framework. As will be seen, this very clear symmetry difference between anion types forms a basis for

understanding the quite different crystal physics of $(\text{TMTSF})_2\text{X}$ salts when X is drawn from one of the two anion subsets.

The crystalline motif universally adopted by the $(\text{TMTSF})_2\text{X}$ salts is illustrated in Figs. 3 and 4. The basic features of the motif can be summarized as follows: (a) zig-zag columns of TMTSF cations extend along the **a** axis of a triclinic (space symmetry group $\text{P}\bar{1}$)¹⁴ unit cell; (b) intracolumnar (**a** axis) and intercolumnar (**b** axis) interactions are dominated by interdonor contacts between selenium atoms that are commonly shorter than a van der Waals distance;¹⁵ and (c) alternate sheets of donor columns are coupled along the **c** axis via planes of anions that exhibit various types and degrees of disorder. At high temperature, the anions are required by space group symmetry to lie on special positions that demand centrosymmetry. For octahedral anions, this does not impose any additional symmetry elements nor does it require positional disorder. For tetrahedral anions (see above), positional disorder is required at high temperature because the point group T_d is noncentrosymmetric. As will become evident, the ordering of tetrahedral anions at low temperature plays a major role in the crystal physics of these materials.

To progress further, it is essential to have some measure of size, as well as symmetry, for the set of anions found in the $(\text{TMTSF})_2\text{X}$ salts. To this end, a very simple van der Waals-like set of spherical anion radii (herein R_1^{vdW}) has been derived.¹⁶ A general example, the PF_6^- anion, will be given in detail for clarity. A mean P–F bond length (1.70 angstroms, $R_{\text{P-F}}$ of Fig. 2) was determined from a literature survey. Pauling's¹⁵ van der Waals radius for fluorine (1.35 angstroms, $R_{\text{F}}^{\text{vdW}}$ of Fig. 2) was added to the mean bond length to yield the hexafluorophosphate anion radius ($R_{\text{P-F}} + R_{\text{F}}^{\text{vdW}} = R_1^{\text{vdW}} = 2.95$ angstroms).

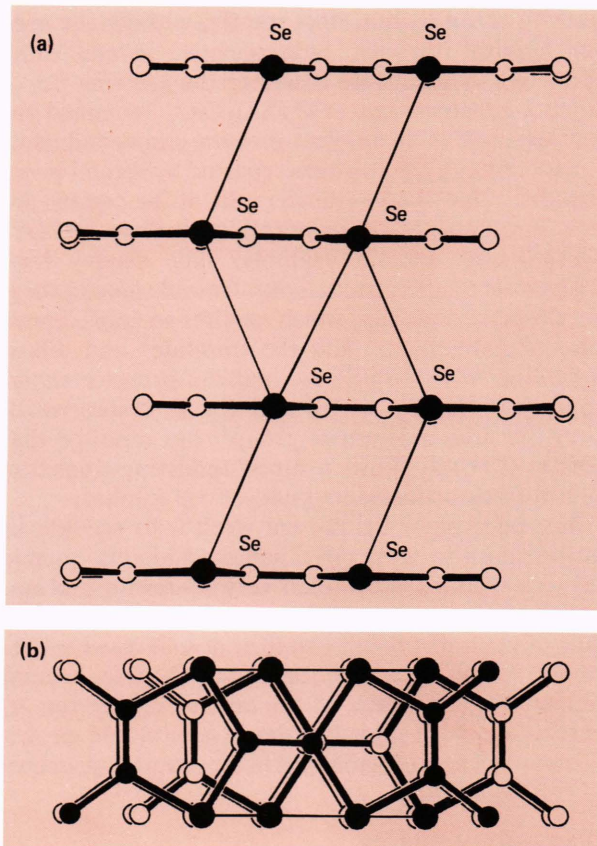
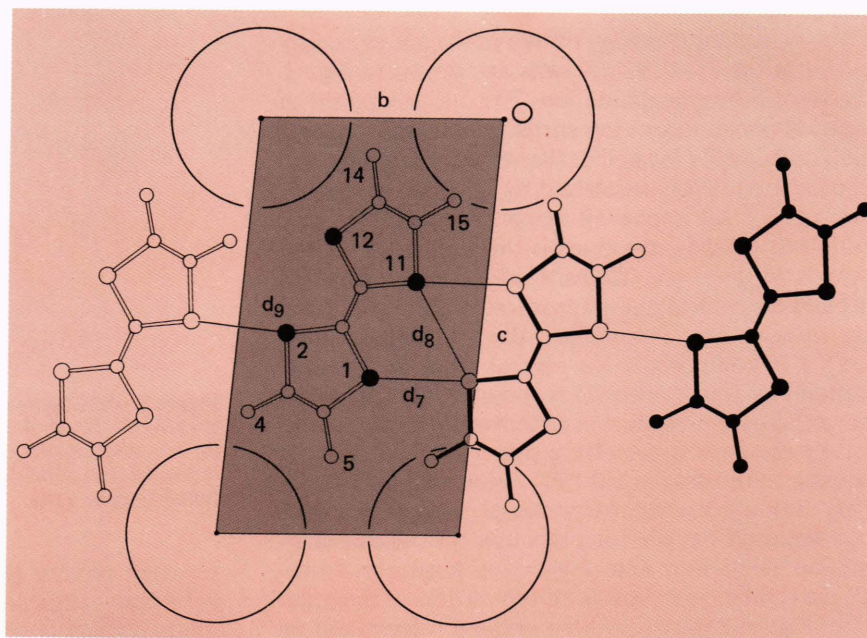


Figure 3—(a) An isolated columnar array of TMTSF donors as found in the crystal structure of the $(\text{TMTSF})_2\text{X}$ salts. Thin lines denote intracolumnar interactions between selenium atoms. (b) Molecular overlap pattern within the columnar array of TMTSF donors.

An analogous procedure can be applied to all anions of the set, yielding an R_1^{vdW} of 2.84 angstroms for the perchlorate anion, for example.

Figure 4—The (100) projection of the crystal structure for all known $(\text{TMTSF})_2\text{X}$ salts. Large circles indicate the average positions of the counterion X, while thin lines (labeled d_7 , d_8 , and d_9) denote short interdonor contacts between selenium atoms.



To provide a clear illustration of the effects of anion size and symmetry on a structural parameter, the variation of the length of the *c* axis (the direction along which planes of donor cations and complex anions alternate; see Fig. 3) over a series of $(\text{TMTSF})_2\text{X}$ salts¹⁷ is considered in Fig. 5. It is immediately obvious that separate, nominally linear correlations are required for salts with octahedral and tetrahedral anions. Clearly, then, anion size and symmetry are crucial considerations in any detailed analysis of the crystal physics of the materials. It is to be noted that variations with anion size and symmetry (a) in the magnitude of the *b* axis,¹⁶ (b) in parameters related to the *a* axis length,¹⁸ (c) in cell volume, and (d) in the selenium atom-selenium atom contact distances¹⁹ have also been reported. In general, however, trends in these parameters are severely muted (as is expected, given the crystalline motif) in comparison to the rather dramatic results illustrated in Fig. 5.

Another aspect of the crystal physics of these materials in which anion size and symmetry bear careful examination concerns the coupling of the anions to the TMTSF donor framework. It has been noted^{20,21} that the structural cavity in which the anion resides in the $(\text{TMTSF})_2\text{X}$ salts is primarily composed of the terminal methyl groups of the TMTSF donor. There is also a pair of selenium atoms from centrosymmetrically related TMTSF cations that are involved in the definition of the structural cavity. The distribution of methyl groups and selenium atoms about the average position of the anion, X, is illustrated in Fig. 6. Although this array is only required by crystallographic symmetry to be centrosymmetric, the actual distribution of methyl groups is that of a skewed, trigonal antiprism (point symmetry group D_{3d}),¹² with the selenium atoms capping the trigonal faces.

Of particular importance has been the recognition^{20,21} that, while the cavity geometry is largely invariant across the series of $(\text{TMTSF})_2\text{X}$ salts, anions of different symmetries adopt different orientations within the cavity. It is interesting to consider the matchup between the geometrical features of the anion cavity and the symmetry axes for octahedral and tetrahedral anions. In Fig. 7, the hexafluoroarsenate, AsF_6^- , anion is oriented in its structural cavity on the basis of its crystal structure. From the four projection views of Fig. 7, it is evident that each methyl group interaction vector lies qualitatively parallel to one of the threefold (rotation by 120 degrees) symmetry axes of the AsF_6^- octahedron, while the selenium atom interaction vector lies close to a fourfold (rotation by 90 degrees) symmetry axis. On the whole, the geometry of the structural cavity seems remarkably well suited to the accommodation of an anion of octahedral symmetry, which probably accounts in detail for the absence of positional disorder for salts with octahedral anions. In that same vein, trends in the interaction distances (measured from a methyl carbon or selenium atom to the center of mass of the anion) R_4 , R_{14} , R_{15} , and R_{Se} for salts with octahedral anions are illustrated in Fig. 8. For the limited data available, all

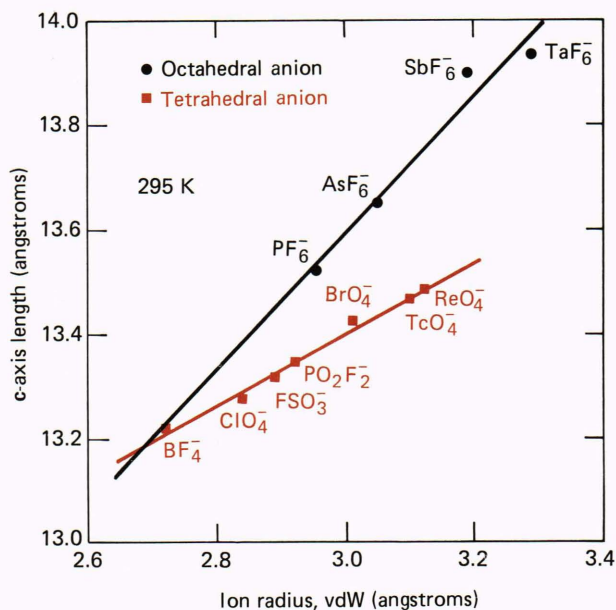


Figure 5—Plot of the *c*-axis length (in angstroms) versus anion radius (R_1^{vdW}) for salts with octahedral and tetrahedral anions.

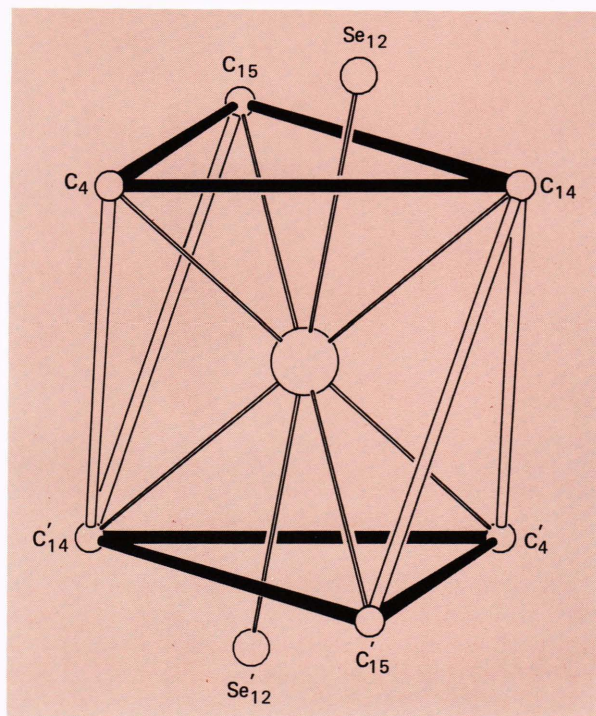


Figure 6—Geometry of the structural cavity about the anion X in the $(\text{TMTSF})_2\text{X}$ salts. Primed atoms are related to unprimed atoms by inversion symmetry.

interaction distances appear to vary linearly with anion size.

Turning to salts with tetrahedral anions, it is unlikely (recalling the essentially invariant geometry of the structural cavity) that a similar symmetry match can

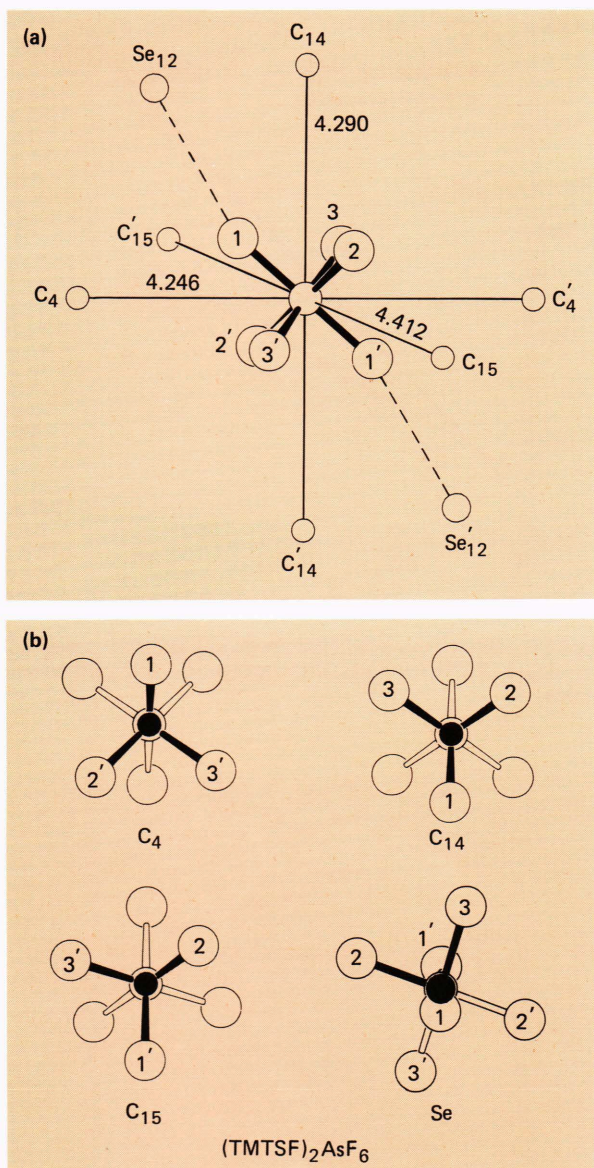


Figure 7—(a) Disposition of methyl groups and selenium atoms about the AsF_6^- anion in $(\text{TMTSF})_2\text{AsF}_6$. (b) Projection views down the R_4 , R_{14} , R_{15} , and R_{Se} interaction vectors.

be anticipated. That intuition is extended in Fig. 9, where views of the disordered perchlorate anion within its crystalline cavity are presented. From Fig. 9, it is evident that the $\text{C}_4 \dots \text{C}'_4$ and $\text{C}_{14} \dots \text{C}'_{14}$ interaction vectors closely parallel twofold (rotation by 180 degrees) symmetry axes of the ClO_4^- anion, irrespective of the anion orientation. (Equivalently, these interaction vectors closely follow fourfold symmetry axes of the cube defined by the disordered oxygen ions.) The striking aspect of Fig. 9 is the absence of near colinearity of the $\text{C}_{15} \dots \text{C}'_{15}$ and $\text{Se}_{12} \dots \text{Se}'_{12}$ interaction vectors and of any of the symmetry axes of the individual perchlorate anions or their composite cube. Thus, it is the latter two interactions that probably induce anion ordering as the cavity contracts when the temperature is lowered. In that same context, the variation

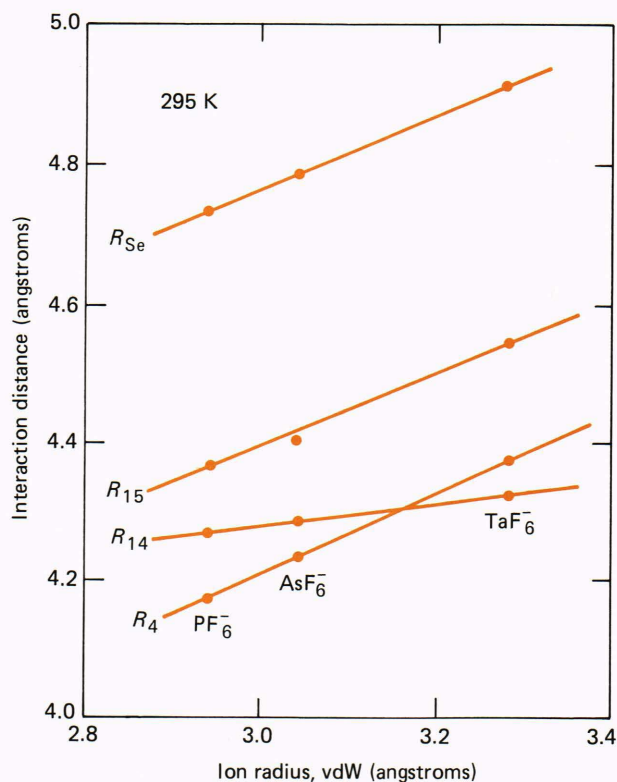


Figure 8—Variation of the interaction distances R_4 , R_{14} , R_{15} , and R_{Se} with anion radius (R_1^{vdW}) for salts with octahedral anions.

in the magnitude of the interaction vectors with anion size is quite different for salts with tetrahedral anions than for salts with octahedral anions (compare Figs. 8 and 10). Here, only the interaction distances R_4 and R_{15} appear to be linear variables of R_1^{vdW} . The rather interesting behavior of R_{Se} is to be noted, and it is recalled that this is one of the interaction vectors that probably promote anion ordering.

Before leaving the $(\text{TMTSF})_2\text{X}$ salts, two further points will be developed: (a) a means by which the fit of the anion to its observed cavity can be determined and (b) the role of anion ordering in salts with tetrahedral anions and the onset of a metal-insulator phase transition. These two points are intimately linked because the fit of the anion to its structural cavity is most likely related to its propensity to order, and, in general, the anion-ordering and metal-insulator transition temperatures are coincident. It has also become evident that anion ordering is a prerequisite for achieving a superconducting ground state.²²

A very simple scheme to measure the fit of the anion to its structural cavity has been proposed elsewhere²³ and is outlined here. Its implementation requires only the ion radius (R_1^{vdW}), the van der Waals radius of a methyl group ($R_{\text{Me}}^{\text{vdW}}$) (given by Pauling¹⁵), and some consistent measure of the cavity radius ($R(C)$). As described above, the surface of the structural cavity is largely composed of methyl groups and selenium atoms from TMTSF donors. Furthermore, the methyl group interaction vector R_4 is quite short

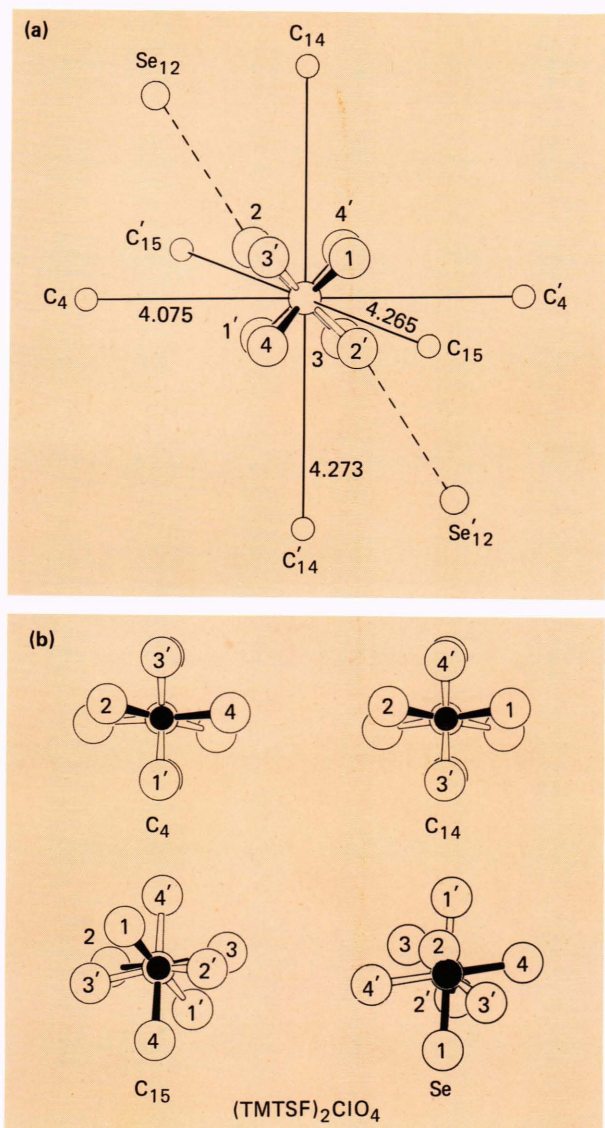


Figure 9—(a) Disposition of methyl groups and selenium atoms about the disordered ClO_4^- anion in $(\text{TMTSF})_2\text{ClO}_4$. (b) Projection views down the R_4 , R_{14} , R_{15} , and R_{Se} interaction vectors.

in all salts (see Figs. 8 and 10) and, importantly, shows a common functional dependence on R_1^{vdW} for both subsets of anions. Thus, R_4 will be taken as a consistent measure of the cavity radius. Quantitatively, the fit of the anion to its structural cavity can be evaluated as follows: $\Delta R_4(C) = R_4 - (R_1^{\text{vdW}} + R_{\text{Me}}^{\text{vdW}})$, where $\Delta R_4(C)$ is, in effect, a measure of the overlap of the van der Waals sphere of the complex anion X and the interacting methyl group separated by the distance R_4 . Increasingly more negative values of $\Delta R_4(C)$ signify a tighter fit of the anion within its cavity and an increasing tendency to order. Plots of $\Delta R_4(C)$ versus R_1^{vdW} for salts with octahedral and tetrahedral anions are presented in Fig. 11. It is immediately recognized that separate, nominally linear variations of $\Delta R_4(C)$ with R_1^{vdW} are required for salts with octahedral and tetrahedral anions. It has also

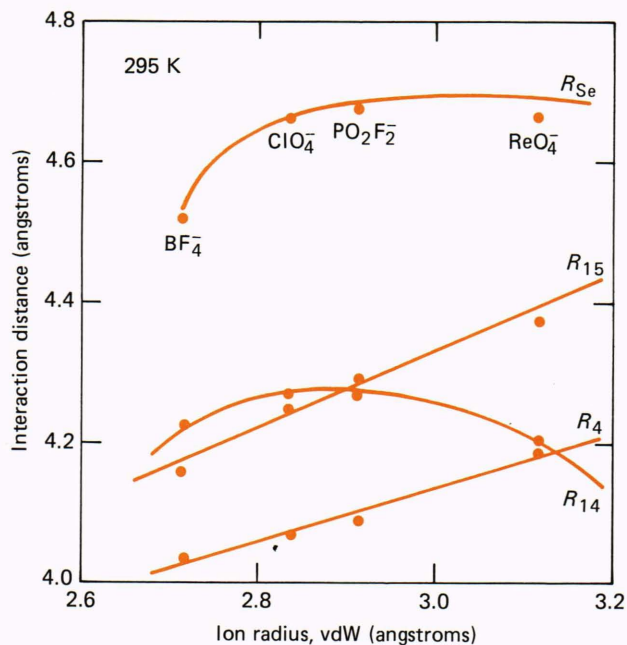


Figure 10—Variation of the interaction distances R_4 , R_{14} , R_{15} , and R_{Se} with anion radius (R_1^{vdW}) for salts with tetrahedral anions.

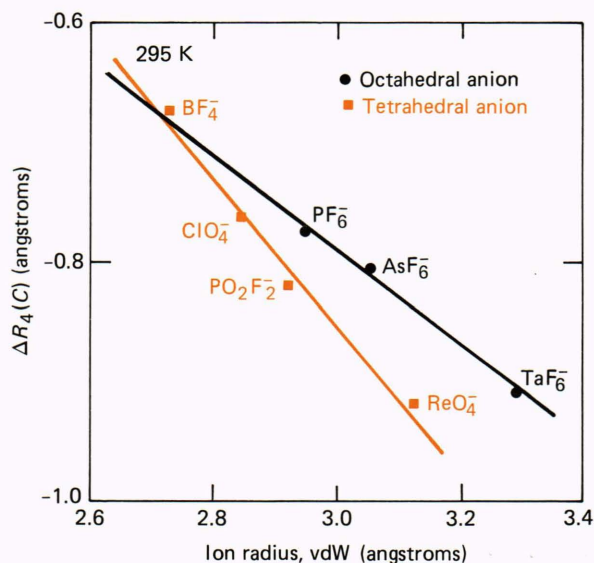


Figure 11—Plots of $\Delta R_4(C)$ versus anion radius (R_1^{vdW}) for salts with octahedral and tetrahedral anions.

been suggested²³ that the generally more negative value of $\Delta R_4(C)$ for a given value of R_1^{vdW} for salts with tetrahedral anions signals a stronger anion-donor interaction.

Moreover, for salts with tetrahedral anions, the increasingly negative values for $\Delta R_4(C)$ generally parallel the increase in anion-ordering (and metal-insulator) transition temperature, which is 87 K for $(\text{TMTSF})_2\text{FSO}_3$, 135 K for $(\text{TMTSF})_2\text{PO}_2\text{F}_2$, and 180 K for $(\text{TMTSF})_2\text{ReO}_4$.²⁴ Because anion ordering has been strongly linked to the metal-insulator transi-

tion, it is to be anticipated that the metal-insulator transition temperature will depend on anion size for salts with tetrahedral anions. This perception is borne out in Fig. 12, where the metal-insulator transition temperature (T_{M-I}) is seen to increase monotonically with R_1^{vdW} for $(\text{TMTSF})_2\text{X}$ salts with tetrahedral anions. A very similar trend is also found for the isostructural $(\text{TMTTF})_2\text{X}$ salts (where TMTTF is the sulfur analog of TMTSF)²⁵ with tetrahedral anions, also shown in Fig. 12. The virtual absence of any trend in T_{M-I} with anion size for salts with octahedral anions (Fig. 12) can be traced to the absence of positional disorder in those salts and to the fact that the driving force for the metal-insulator transition for this subset of anions is the condensation of a spin-density wave. This is a phenomenon that is strongly dependent on the coupling of the spins of the conduction electrons to the phonon background²⁴ but is virtually independent of anion parameters.

It is, of course, the exceptions to this general trend for salts with tetrahedral anions that are potentially the most interesting. The ambient-pressure superconducting salt $(\text{TMTSF})_2\text{ClO}_4$ does not follow this general relationship, in that the anion-ordering temperature (24 K) is well below that expected (80 K) on the basis of the size of the perchlorate anion, and there is only a weak anomaly at that temperature in high-resolution resistivity data.²⁶

$(\text{BEDT-TTF})_2\text{X}$ SALTS

The molecular structure of the electron donor BEDT-TTF is presented in Fig. 13. In addition to the obvious substitution of sulfur atoms for selenium atoms in the tetrachalcogenoethylene core, this donor has additional heteroatom sites near the perimeter of the molecule that also contribute to the interdonor interactions in its salts.²⁷ Many of the same anions in the $(\text{TMTSF})_2\text{X}$ system have also been used in forming $(\text{BEDT-TTF})_2\text{X}$ salts. There are, however, some important additions (Fig. 14), particularly those of the linear triiodide (I_3^-) and dibromiodide (IBr_2^-) anions whose salts are ambient-pressure superconductors.^{8,9} Immediately, then, one recognizes that there will be differences between the solid-state physics of the $(\text{BEDT-TTF})_2\text{X}$ salts and the $(\text{TMTSF})_2\text{X}$ salts in that the salt that is an ambient pressure superconductor in the TMTSF series is the noncentrosymmetric perchlorate anion, while the analogous salts in the BEDT-TTF materials contain the centrosymmetric triiodide and dibromiodide anions (symmetry point group $D_{\infty h}$).¹²

However, in a broad structural sense, these two families of materials are quite similar. Columnar arrays of BEDT-TTF cations (Fig. 15) are assembled into a layered structure (Fig. 16) that is reminiscent of the structural motif adopted by the $(\text{TMTSF})_2\text{X}$ salts. Two contrasting points have emerged. First, within the $(\text{TMTSF})_2\text{X}$ system, salts with noncentrosymmetric anions show disorder at high temperature, and disorder/order transitions play a prominent role in the low-temperature physics of the materials (see above); in

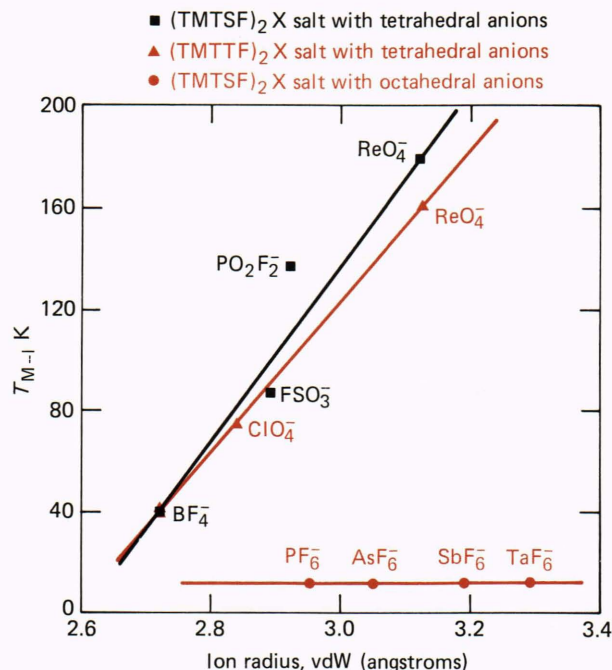


Figure 12—Variation of metal-insulator transition temperature (T_{M-I}) with anion radius (R_1^{vdW}) for (a) four $(\text{TMTSF})_2\text{X}$ salts with tetrahedral anions, (b) three $(\text{TMTTF})_2\text{X}$ salts with tetrahedral anions, and (c) four $(\text{TMTSF})_2\text{X}$ salts with octahedral anions.

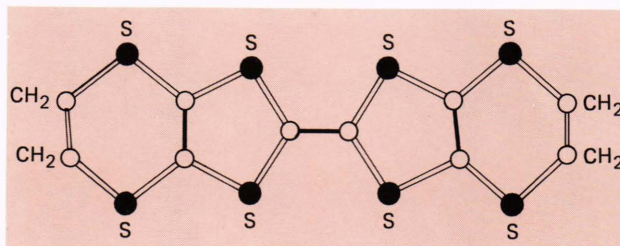


Figure 13—Molecular structure of the electron donor BEDT-TTF. Shaded bonds indicate formal carbon-carbon double bonds.

contrast, anion ordering at high temperature is the general rule for $(\text{BEDT-TTF})_2\text{X}$ salts, regardless of anion symmetry. Second, all high-temperature phases of the $(\text{TMTSF})_2\text{X}$ salts are isostructural (triclinic), but there is a diversity of high-temperature structural types for the $(\text{BEDT-TTF})_2\text{X}$ salts that encompasses monoclinic and orthorhombic space group symmetries as well as triclinic. In fact, some $(\text{BEDT-TTF})_2\text{X}$ salts even crystallize in two different structural phases (herein called α and β) with deviant electrical properties.²⁷

It has recently been determined,²⁸ however, that the apparently unrelated structural diversity for the $(\text{BEDT-TTF})_2\text{X}$ salts can be unified by the application of the well-known principle of substructures and superstructures. To that end, a parent subcell can be defined that is centrosymmetric, is of triclinic symmetry, and has cell dimensions of the following magnitudes: $|\mathbf{a}| \approx 8$ to 9 angstroms (the donor stacking

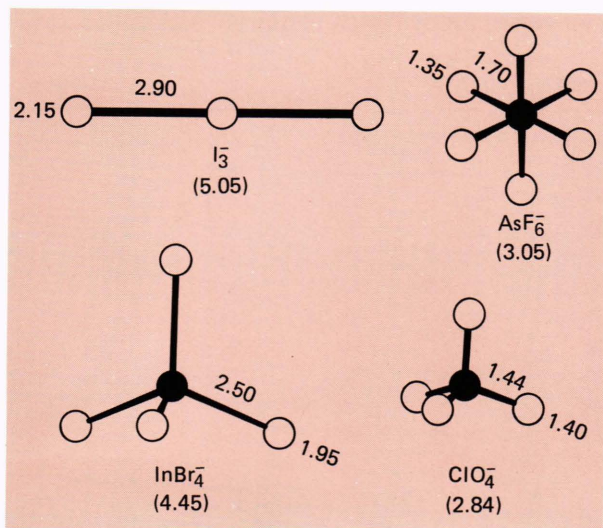


Figure 14—Molecular geometry and dimensions (in angstroms) for several anions used in the series of (BEDT-TTF)₂X salts.

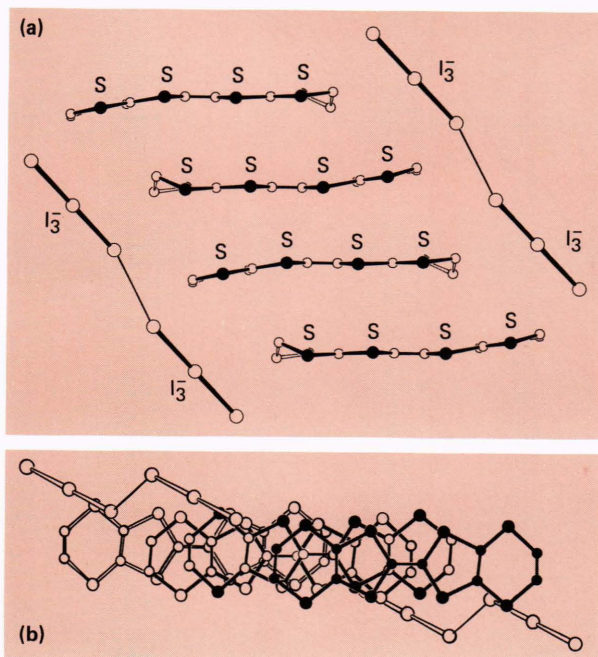


Figure 15—(a) A columnar array of BEDT-TTF donors along with its contiguous chains of triiodide anions in the structure of α -(BEDT-TTF)₂I₃. (b) Molecular overlap pattern within the columnar array of BEDT-TTF donors.

axis), $|b| \approx 6$ to 7 angstroms (the interstacking axis), and $|c| \approx 14$ to 19 angstroms (the propagation axis for the interleaved planes of donors and anions). The rather liberal ranges assigned to the cell vectors (especially to c) of the parent subcell are dictated by the influence of anion size and symmetry and the presence, in some instances, of solvent molecules within the anion layers. The crystal structures of 11 of the 12 reported (BEDT-TTF)₂X salts²⁷ can be assigned to this parent subcell or to one of its first-generation (dou-

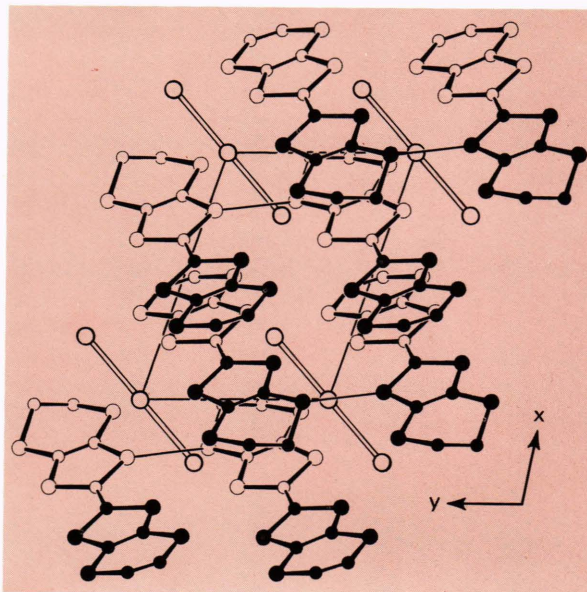


Figure 16—The (001) projection of the crystal structure of α -(BEDT-TTF)₂I₃. Thin lines denote interdonor contacts between sulfur atoms.

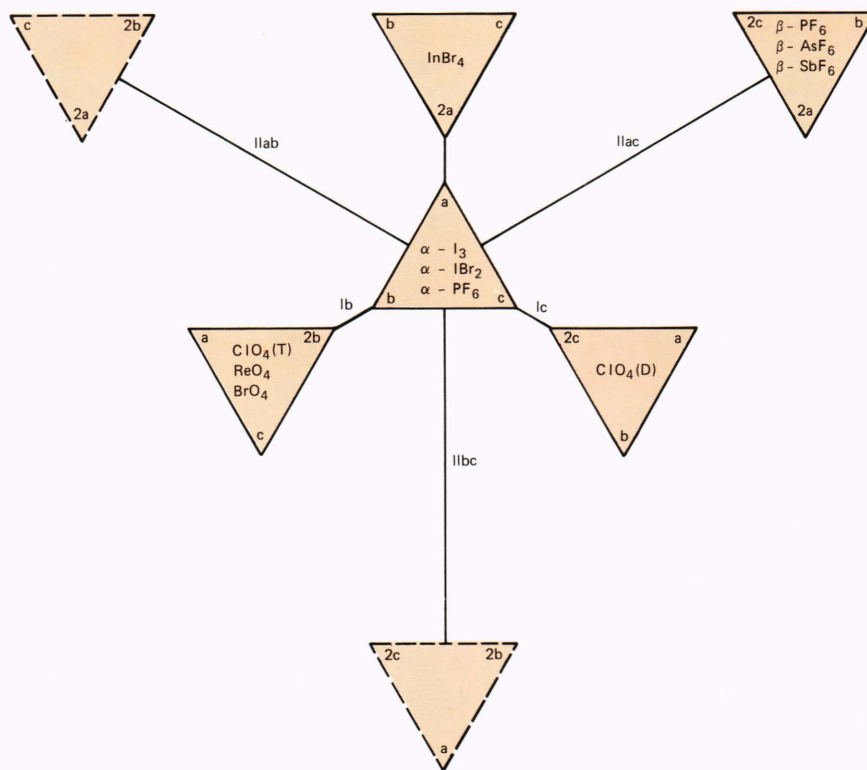
bling of any one subcell vector) or second-generation (doubling of any two subcell vectors) supercells. Table 1 presents unit-cell data for the 11 (BEDT-TTF)₂X salts; Fig. 17 is a pictorial representation of the structural heritage of the salts displayed as a crystallographic family tree.

A brief study of the family tree of Fig. 17 reveals several aspects of the structural lineage.

1. The parent subcell is populated by three salts with centrosymmetric anions: the α -polymorphs of (BEDT-TTF)₂I₃ and (BEDT-TTF)₂IBr₂, ambient-pressure superconductors; and the α -form of (BEDT-TTF)₂PF₆, a small band-gap semiconductor.
2. All first-generation supercells (Ia(2abc), Ib(a2bc), and Ic(ab2c)) are populated by salts with noncentrosymmetric tetrahedral anions, a clear indication of the influence of anion symmetry. A plethora of electrical behavior is displayed by the first-generation progeny: small band-gap semiconductors populate supercells Ia (the tetrabromoindate, InBr₄⁻, salt) and Ic (the dioxane (D) solvate of the perchlorate salt), while the Ib supercell contains the trichloroethane (T) solvate of the perchlorate salt (a two-dimensional semimetal with metallic conductivity to 1.4 K) and the perrhenate salt (a high-temperature ($T > 81$ K) metal with an insulating or superconducting low-temperature ground state, depending on applied pressure).
3. At present, the lone occupied second-generation supercell (IIac(2ab2c)) is populated by three salts with centrosymmetric anions, the β -forms of (BEDT-TTF)₂PF₆, (BEDT-TTF)₂AsF₆, and (BEDT-TTF)₂SbF₆, all of which are high-

Table 1—Systematized structural data for several (BEDT-TTF)₂X salts.

Salt	Supercell	a (Å)	b (Å)	c (Å)	α (deg)	β (deg)	γ (deg)	V(Å ³)	Space Group
α-I ₃		9.100	6.615	15.286	95.59	94.38	109.78	856	P $\bar{1}$
α-IBr ₂		8.975	6.593	15.093	94.97	93.79	110.54	829	P $\bar{1}$
α-PF ₆		8.597	6.462	14.711	97.64	98.87	95.71	794	P $\bar{1}$
InBr ₄	(Ia)	17.470	6.618	16.040	92.43	95.29	99.12	1820	P $\bar{1}$
ClO ₄ (T)	(Ib)	7.740	12.966	18.620	110.85	100.68	75.20	1684	P $\bar{1}$
ReO ₄	(Ib)	7.798	12.579	17.102	106.63	99.65	88.97	1584	P $\bar{1}$
BrO ₄	(Ib)	7.795	12.613	17.148	107.03	99.56	88.74	1589	P $\bar{1}$
ClO ₄ (D)	(Ic)	8.242	6.677	32.998	90	92.71	90	1814	P2/c
β-PF ₆	(IIac)	14.960	6.664	32.643	90	90	90	3256	Pnan
β-AsF ₆	(IIac)	14.890	6.666	35.379	90	111.20	90	3274	A2/a
β-SbF ₆	(IIac)	14.93	6.70	33.56	90	93.88	90	3349	I2/a

Figure 17—Crystallographic family tree for the (BEDT-TTF)₂X salts.

temperature metals with a sharp metal-insulator transition near room temperature (293, 264, and 273 K, respectively).

The symmetry properties of the family tree are particularly illuminating, with alternate generations populated by anions of opposite inversion symmetry. In addition, the spectacular richness of the high-temperature crystallographic lineage for the (BEDT-TTF)₂X salts stands in contrast to the relative starkness of the structural pedigree of the (TMTSF)₂X system. It has been suggested²⁸ that the relative opulence of the structural physics of the (BEDT-TTF)₂X salts stems from the much weaker interdonor (both intracolumnar and intercolumnar) interaction potential in this sulfur-based system and the attendant increase in the flexi-

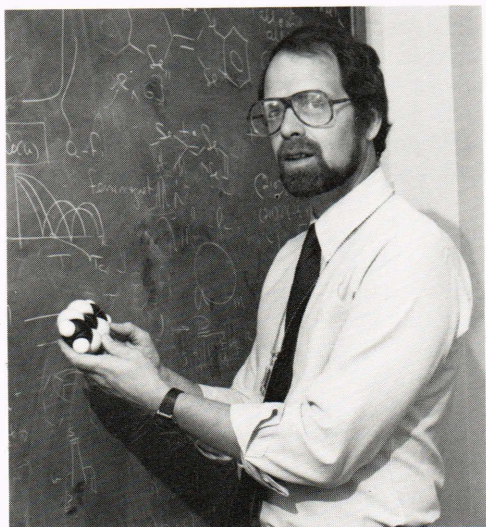
bility of the response of the donor sheets to the structural (size and symmetry) and electronic properties of the charge-compensating anions.

REFERENCES and NOTES

- See, for example, L. R. Melby, R. J. Harder, W. R. Hertler, W. Mahler, R. E. Benson, and W. E. Mochel, "Substituted Quinodimethans. II. Anion-Radical Derivatives and Complexes of 7,7,8,8-Tetracyanoquinodimethan," *J. Am. Chem. Soc.* **84**, 3374 (1962).
- J. Ferraris, D. O. Cowan, V. Walatka, and J. H. Perlstein, "Electron Transfer in a New Highly Conducting Donor-Acceptor Complex," *J. Am. Chem. Soc.* **95**, 948 (1973); L. B. Coleman, M. J. Cohen, D. J. Sandman, F. G. Yamagishi, A. F. Garito, and A. J. Heeger, "Superconducting Fluctuations and the Peierls Instability in an Organic Solid," *Solid State Commun.* **12**, 1125 (1973).
- T. J. Kistenmacher, T. E. Phillips, and D. O. Cowan, "The Crystal Structure of the 1:1 Radical Cation-Radical Anion Salt of 2,2'-Bis-1,3-dithiole (TTF) and 7,7,8,8-Tetracyanoquinodimethane (TCNQ)," *Acta Crystallogr.* **B30**, 763 (1974).

- ⁴K. Bechgaard, C. S. Jacobsen, K. Mortensen, H. J. Pedersen, and N. Thorup, "The Properties of Five Highly Conducting Salts: (TMTSF)₂X, X = PF₆⁻, AsF₆⁻, SbF₆⁻, BF₄⁻, and NO₃⁻, Derived from Tetramethyltetraselenafulvalene (TMTSF)," *Solid State Commun.* **33**, 1119 (1980).
- ⁵D. Jerome, A. Mazaud, M. Ribault, and K. Bechgaard, "Superconductivity in a Synthetic Organic Conductor (TMTSF)₂PF₆," *J. Phys. (Paris) Lett.* **41**, L95 (1980).
- ⁶K. Bechgaard, K. Carneiro, F. B. Rasmussen, M. Olsen, G. Rindorf, C. S. Jacobsen, and H. J. Pedersen, "Superconductivity in an Organic Solid. Synthesis, Structure, and Conductivity of Bis(tetramethyltetraselenafulvalenium) Perchlorate, (TMTSF)₂ClO₄," *J. Am. Chem. Soc.* **102**, 2440 (1981).
- ⁷S. S. P. Parkin, E. M. Engler, R. R. Schumaker, R. Lagier, V. Y. Lee, J. C. Scott, and R. L. Greene, "Superconductivity in a New Family of Organic Conductors," *Phys. Rev. Lett.* **50**, 270 (1983).
- ⁸E. B. Yagubskii, I. F. Schegolev, V. N. Laukhin, P. A. Konoнович, M. V. Kartsovnik, A. V. Zvarykina, and L. I. Buravov, "Normal-Pressure Superconductivity in an Organic Metal (BEDT-TTF)₂I₃[Bis(Ethylene Dithiolo) Tetrathiafulvalene Triiodide]," *Zh. Eksp. Teor. Fiz., Pis'ma Red.* **39**, 12 (1984).
- ⁹J. M. Williams, H. H. Wang, M. A. Beno, T. J. Emge, L. M. Sowa, P. T. Coppins, F. Behroozi, L. N. Hall, K. D. Carlson, and G. W. Crabtree, "Ambient-Pressure Superconductivity at 2.7 K and Higher Temperatures in Derivatives of (BEDT-TTF)₂IBr₂: Synthesis, Structure, and Detection of Superconductivity," *Inorg. Chem.* **23**, 3839 (1984).
- ¹⁰M. Mizuno, A. F. Garito, and M. P. Cava, "'Organic Metals': Alkylthio Substitution Effects in Tetrathiafulvalene-Tetracyanoquinodimethane Charge-Transfer Complexes," *J. Chem. Soc. Chem. Commun.* **18** (1978); W. P. Krug, A. N. Bloch, T. O. Poehler, and D. O. Cowan, "A New π -Donor for the Study of Organic Metals," *Ann. N. Y. Acad. Sci.* **313**, 366 (1978).
- ¹¹K. Murata, M. Tokumoto, H. Anzai, H. Bando, G. Saito, K. Kajimura, and T. Ishiguro, "Superconductivity with the Onset at 8 K in the Organic Conductor β -(BEDT-TTF)₂I₃ under Pressure," *J. Phys. Soc. (Japan)* **54**, 1236 (1985).
- ¹²For an elementary discussion of group theory applied to molecular systems, see F. A. Cotton, *Chemical Applications of Group Theory*, John Wiley Interscience, New York (1964).
- ¹³Tetrahedral is used in its broadest sense here to describe all salts containing four-coordinate anions. The term can be applied in the strictest sense to the tetrafluoroborate (BF₄⁻), perchlorate (ClO₄⁻), perbromate (BrO₄⁻), pertechnetate (TcO₄⁻), and perhenate (ReO₄⁻) anions but only in a general sense to the lower symmetry fluorosulfate (FSO₃⁻) and difluorophosphate (PO₂F₂⁻) anions.
- ¹⁴An introduction to crystal symmetry and space groups can be found in M. J. Buerger, *Elementary Crystallography*, MIT Press, Cambridge (1978).
- ¹⁵L. Pauling, *The Nature of the Chemical Bond*, Cornell University Press, Ithaca (1960).
- ¹⁶T. J. Kistenmacher, "Anion Symmetry and the Separability of Structural Parameters for Tetramethyltetraselenafulvalenium Salts, (TMTSF)₂X," *Mol. Cryst. Liq. Cryst.* (in press).
- ¹⁷Appropriate references to the primary literature for the structural and electrical properties of the (TMTSF)₂X salts can be found in Ref. 18 and in references cited therein.
- ¹⁸T. J. Kistenmacher, "Anion Size and the Structural Properties of (TMTSF)₂X Salts: Intracolumnar Effects," *Solid State Commun.* **51**, 275 (1984).
- ¹⁹J. M. Williams, M. A. Beno, J. C. Sullivan, L. M. Banovetz, J. M. Braam, G. S. Blackman, C. D. Carlson, D. L. Greer, D. M. Loesing, and K. Carneiro, "Role of Monovalent Anions in Organic Superconductors," *Phys. Rev.* **B28**, 2873 (1983).
- ²⁰M. A. Beno, G. S. Blackman, P. C. W. Leung, and J. M. Williams, "Hydrogen Bond Formation and Anion Ordering in Superconducting (TMTSF)₂ClO₄ and (TMTSF)₂AsF₆," *Solid State Commun.* **48**, 99 (1983).
- ²¹T. J. Kistenmacher, "Anion-Donor Coupling in (TMTSF)₂X Salts: Symmetry Considerations," *Solid State Commun.* **51**, 931 (1984).
- ²²P. Garoche, R. Brusetti, and K. Bechgaard, "Influence of the Cooling Rate on the Superconducting Properties of the Organic Solid Di-Tetramethyltetraselenafulvalenium-Perchlorate, (TMTSF)₂ClO₄," *Phys. Rev. Lett.* **49**, 1346 (1982).
- ²³T. J. Kistenmacher, "Cavity Size versus Anion Size in (TMTSF)₂X Salts: Possible Implications for the Uniqueness of (TMTSF)₂ClO₄," *Solid State Commun.* **50**, 729 (1984).
- ²⁴For a very recent review, see R. L. Greene and G. B. Street, "Conducting Organic Materials," *Science* **226**, 651 (1984).
- ²⁵C. Coulon, P. Delhaes, S. Flandrois, R. Lagnier, E. Bonjour, and J. M. Fabre, "A New Survey of the Physical Properties of the (TMTTF)₂X Series. Role of the Counterion Ordering," *J. Phys. (Paris)* **43**, 1059 (1982).
- ²⁶D. U. Gubser, W. W. Fuller, T. O. Poehler, J. Stokes, D. O. Cowan, M. Lee, and A. N. Bloch, "Resistive and Magnetic Susceptibility Transitions in Superconducting (TMTSF)₂ClO₄," *Mol. Cryst. Liq. Cryst.* **79**, 225 (1982).
- ²⁷Appropriate references to the primary literature for the structural and electrical properties of the (BEDT-TTF)₂X salts can be found in Ref. 28 and in references cited therein.
- ²⁸T. J. Kistenmacher, "Structural Systematics in the Family of (BEDT-TTF)₂X Salts," *Solid State Commun.* **53**, 831 (1985).

ACKNOWLEDGMENT — Support of this research by the National Science Foundation under Grant No. DMR-8307693 is gratefully acknowledged.



THE AUTHOR

THOMAS J. KISTENMACHER is a senior staff chemist in the Milton S. Eisenhower Research Center. He obtained a B.S. degree in chemistry from Iowa State University and M.S. and Ph.D. degrees in chemistry from the University of Illinois. During 1969-71, he was a Junior Fellow in chemical physics at the California Institute of Technology. During 1971-82, he served on the faculties of The Johns Hopkins University and the California Institute of Technology. Dr. Kistenmacher joined APL in 1982 as a member of the Microwave Physics Group. In 1984, he became a member of the Materials Science Group, where his current research interests include crystalline structure and structure-physical property relationships in highly conductive organic solids, local structure and magnetic properties of amorphous thin films and multilayers, and the elucidation of structural models for icosahedral materials.